# Band Gap Narrowing vs. Formation of Electronic States in the Gap in N-TiO2 Thin Films



| | |
|---|---|
| Journal: | *The Journal of Physical Chemistry* |
| Manuscript ID: | jp-2010-04634j.R2 |
| Manuscript Type: | Article |
| Date Submitted by the Author: | 17-Oct-2010 |
| Complete List of Authors: | Romero-Gomez, Pablo; Instituto de Ciencia de Materiales de Sevilla, Superficies, Interfases y Capas Finas<br>Said, Hamad; University Pablo de Olavide, Department of Physical, Chemical and Natural Systems<br>Gonzalez, Juan; Instituto de Ciencia de Materiales de Sevilla, Superficies, Interfases y Capas Finas<br>Barranco, Angel; Instituto de Ciencia de Materiales de Sevilla, Surfaces Interfaces and Thin Films<br>Espinós, Juan P.; Instituto de Ciencia de Materiales de Sevilla, Surfaces Interfaces and Thin Films<br>Cotrino, Jose; Universidad de Sevilla, Instituto de Ciencia de Materiales<br>Gonzalez-Elipe, Agustín; Instituto de Ciencia de Materiales de Sevilla (CSIC-Univ. Sevilla), Superficies, Interfases y Capas Finas |
| | |

# Band gap narrowing vs. formation of electronic states in the gap in N-$TiO_2$ thin films

P. Romero-Gómez[1], Said Hamad[3], J.C. González[1], A. Barranco[1], J.P. Espinós[1], J. Cotrino[1,2], A.R. González-Elipe[1*]

*1. Instituto de Ciencia de Materiales de Sevilla (CSIC-Univ. Sevilla). Avda. Américo Vespucio 49. 41092 Sevilla (Spain).* http://www.sincaf-icmse.es

*2. Departamento de Física Atómica, Molecular y Nuclear. Universidad de Sevilla. Avda. Reina Mercedes 49, 41012 Sevilla. Spain.*

*3. Department of Physical, Chemical and Natural Sciences. Universidad Pablo de Olavide. Carretera de Utrera, km 1. Sevilla. Spain*

*arge@icmse.csic.es

## Abstract

N-containing $TiO_2$ thin films with different amounts of nitrogen have been prepared by plasma enhanced chemical vapor deposition (PECVD) by using different titanium precursors without (titanium isopropoxide, TTIP) and with (tetrakis diethyl amino titanium, TDEAT and tetrakis dimethyl amino titanium, TDMAT) nitrogen in their structures and different $N_2/O_2$ ratios as plasma gas. For low/high content of nitrogen, Ti-NO and/or Ti-N like species have been detected in the films by X-ray photoelectron spectroscopy (XPS). Their optical behavior is characterized by a red shift of their absorption edge when Ti-N species are a majority and by an unmodified edge with localized absorption states in the gap when only Ti-NO like species are present in the film. The experimental results have been interpreted by calculating the density of states of model systems consisting of a 2x2x3 repetition of the anatase unit cell. This basic structure incorporates nitrogen defects in either substitutional or interstitial lattice positions that are considered equivalent to the Ti-N and Ti-NO like species detected by XPS. To simulate the effect of, respectively, a low or a high concentration of nitrogen, calculations have been carried out by placing two nitrogen defects either in separated or in nearby positions of the anatase structure. The computational analysis reveals that the defects have different stabilization energies and confirm that an edge shift of the valence band is induced by the substitutional nitrogen centers, as observed when a high

concentration of Ti-N species becomes incorporated into the films. In agreement with the experimental results, when only Ti-NO like species are detected by XPS no band gap narrowing is obtained by the calculations that predict the appearance of localized electronic states in the gap. The fact that only these latter films present water wetting angle photo-activity when irradiated with visible light supports that the presence of Ti-NO like species is a required condition for visible light photo-activity.

**Keywords:** N-modified $TiO_2$; plasma deposition; optical properties; visible photo-activity; electronic structure; N species

## 1. Introduction

N-modified $TiO_2$ materials have been widely studied during the last years because of the possibility to make them photo-catalytically active under visible light illumination. Since the seminal work of Asahi et al,[1] many papers have appeared in the literature trying to unravel the reasons that sustain this behavior.[2-10] Of particular relevance in this regard are the recent works by Di Valentin et al[11-15] where, by combining theory and experiments mainly by EPR, they show that the species responsible for the visible photo-activity of N-containing $TiO_2$ consist of N atoms located in interstitial lattice positions where it bonds to Ti atoms and interacts with a nearby O ion of the lattice (i.e., a kind of Ti-NO species). This model contrasts with more traditional views linking the visible photo-activity of N-doped $TiO_2$ with the formation of substitutional nitrogen species (i.e., a kind of Ti-N species).[1, 5,16] Another related aspect that has generated much discussion within this topic is the influence of the incorporated nitrogen on the optical properties of the materials, namely in the changes in light absorption due to possible modifications of the band gap of the titanium oxide.[17-21] The appearance of absorption features in the visible region of the spectra of N-containing $TiO_2$ is generally taken as a required but not sufficient condition for visible photo-activity.[22] However, the physical causes of this visible absorption are also controversial, with some authors supporting that the effect of the nitrogen species is to shift the band gap of the titanium oxide towards the visible[17-20] and others claiming that these species do not modify the band gap of the oxide but induce some electronic states in the band gap region that give

rise to localized absorption features close to the absorption edge of the titanium oxide.[11-15, 22-24]

In a recent work on N-doped $TiO_2$ thin films prepared by plasma and evaporation methods, we have shown that while Ti-NO species are able to induce some visible light decrease of the wetting angle of the surface,[22] Ti-N species do not induce any kind of visible light activation. However, for the samples to present photo-catalytic activity towards the photo-degradation of dyes it was required that besides Ti-NO species, the films were crystalline with a mixture of anatase and rutile. In this previous investigation we already noted that the absorption spectra of films with a high content of nitrogen depicted some absorption features in the visible, although no correlation could be established between the nitrogen content and the characteristics of the UV-vis absorption spectra.

As a continuation of this previous work, herein we aim primarily at determining whether each kind of nitrogen species (i.e. Ti-NO or Ti-N) has a specific effect on the physical causes (i.e., gap narrowing or development of localized states in the gap) determining the changes in the absorption spectra of N containing titanium oxide thin films (in the following named in general as N-$TiO_2$ although changes in the Ti/O ratio may occur as a consequence of the development of oxygen vacancies whose formation is related with the incorporation of Ti-N species of nitrogen[25]). We approach this problem firstly by investigating experimentally a series of N-$TiO_2$ thin films where we have systematically changed the type and concentration of nitrogen species. To get such an ample set of samples with different concentrations of nitrogen species we have employed the plasma enhanced chemical vapor deposition (PECVD) procedure and modified systematically the plasma conditions and other working parameters like the type of precursor and temperature of the substrate. Suchan experimental approach has hitherto not been widely used for the preparation of photoactive N-$TiO_2$ thin films, although the preparation of photo-active nanoparticles by atmospheric plasma deposition has been reported.[26] The most common titanium precursor used for the PECVD synthesis of $TiO_2$ thin films is titanium isopropoxide (TTIP),[23, 27-30] although tetrakis dimethyl amino titanium (TDMAT) and tetrakis(diethylamido) titanium (TDEAT)[31-33] are other two precursors which are commonly used in methods of preparation of optical thin films. Therefore, another innovative approach of our work is the use of three titanium precursors (TTIP, TDEAT and TDMAT) with the idea that the

presence of direct Ti-N bonds in the structure of two of them and, very likely, their different reactivity, permit to tune the state of nitrogen in the films and to control film properties such as UV-vis absorption spectra and photo-activity.

To account for the different experimental findings and particularly for the changes in the absorption spectra depending on the type and concentration of nitrogen species in the prepared N-$TiO_2$ thin films, we have theoretically modeled the electronic structure of these materials by calculating the density of states of N-modified anatase for three different types of N defects incorporated in its structure. Modeling the Ti-NO (and Ti-ON as a possible alternative) defect states is done by assuming that N occupies an interstitial position and interacts with both oxygen and titanium ions of the lattice. This species, with nitrogen bearing a formal charge of -1 (i.e., $NO^{3-}$ like species), could be described as a $(NO)_O^t$ defect centre according to the Kröger-Vink notation of defect states in oxides. To simulate the Ti-N species, nitrogen replaces substitutionally an oxygen of the lattice and bonds directly to titanium in a kind of nitride species (i.e. $N^{3-}$ species or $N_O^t$ according to the Kröger-Vink notation). Similar calculations simulating the effect of Ti-N and Ti-NO like species can be found in the works by Di Valentin et al.[11,15] and Graciani et al.[25,34] Herein, besides studying the stability of Ti-ON like species, we have simulated the effect on the optical properties of N-$TiO_2$ materials of the concentration of Ti-N or Ti-NO species, an aspect that had not been addressed in these previous theoretical works. For this purpose, calculations have been carried out by placing two defect states quite separated (i.e., simulating a low concentration of nitrogen) or in nearby positions of the structure (i.e., simulating a high concentration of nitrogen), in this latter case making it possible that the two defect states interact between them as it would be the case in samples with a high concentration of nitrogen species. The density of state calculations (DOS) and particularly the analysis of the partial density of state plots of N, Ti and O have confirmed the experimental findings and show that the incorporation of a high concentration of Ti-N species induces a red shift in the absorption gap of the material, while Ti-NO species do not significantly modify the magnitude of the gap between the valence and conduction bands, but induce the formation of new localized states in the band gap zone of the oxide.

Finally, all these experimental and theoretical results are critically discussed in relation with the actual photo-activity of N-$TiO_2$ materials by analyzing the super-hydrophilic conversion of the surface state of the prepared films under visible light irradiation.

## 2. Experimental

### *2.1 Thin film preparation*

$TiO_2$ and N-$TiO_2$ thin films have been prepared by PECVD in a plasma reactor with a remote configuration. The system, supplied with a microwave plasma source (SLAN, from Plasma Consult, GMBh, Germany) has been described in previous works.[27, 28, 35] It consists of an external 2.45 GHz microwave electron cyclotron resonance (MW-ECR) plasma source coupled to the reaction chamber and separated from it by a grid to avoid the microwave heating of the substrates. Under normal conditions of operation, the grid confines the plasma out of the reaction chamber (remote plasma conditions) where the substrate and the precursor dispenser are located. Titanium tetra-isopropoxide (TTIP), Tetrakis(diethylamido)titanium(IV) (TDEAT) and Tetrakis(dimethylamido)titanium(IV) (TDMAT) were used as titanium precursors. In Figure 1 we show a schematic representation of the structure of these three precursors, showing that four direct Ti-N bonds exist in TDEAT and TDMAT. It is likely that some of them can be preserved during the plasma processing of the N-$TiO_2$ thin films.

The plasma source was operated with a power of 400 W with either pure $O_2$ or mixtures $N_2$+$O_2$ at different proportions of nitrogen from 0 % to 97%. The synthesis of the films was carried out either at 298 K or 523 K, although most reported data corresponds to this latter temperature. Controlled dosing of the precursors was achieved by placing them in a stainless steel recipient heated to 305 K, while oxygen or a $N_2/O_2$ mixture was bubbled through it. Both the bubbling line and the shower-type dispenser used to dose the precursor into the chamber were heated to 373K to prevent any condensation in the tube walls. The total pressure during deposition was $4x10^{-3}$ Torr (normal operation conditions). A deposition rate of approximately 2.5 nm $min^{-1}$ was estimated by means of a quartz crystal monitor for the samples grown at room temperature.

The different plasmas used for deposition of the films were characterized by Optical Emission Spectroscopy (OES). The emission spectrum was analyzed using a 0.5 m CVI/Digikrom DK480 monochromator (CVI Laser Corporation, Albuquerque, NM) with a 1200 grooves/mm grating, spectra resolution of 0.2 nm, and spectral sensitivity ranging from 200 to 900 nm (Hamamatsu R928). The light is collected by a fiber optic,

which is fixed to the monochromator and positioned 4 cm downstream from the source center. The light was collected through a hole in the air cooling ring. It should be noted that the spectroscopic intensities are integrated over the line of sight, thus limiting the spatial resolution.

All the films were deposited simultaneously on a silicon wafer and on quartz plates. The thickness of the prepared samples was estimated by measuring the mass thickness of the films by X-ray fluorescence (XRF) and Rutherford Back Scattering (RBS) or directly from cross section views in the electron microscope (note that for a given sample these two values do not coincide except for completely compact thin films). Most experiments were carried out with films with a thickness of some hundreds of nanometers.

*2.2 Methods of characterization*

The optical properties of the samples were primarily determined by UV-vis absorption spectroscopy (Perkin-Elmer Lambda 12 Spectrometer) for samples prepared on fused silica. The ellipsometric characterization of the N-$TiO_2$ films was carried out in a J.A. Woollam VASE (variable angle spectroscopic ellipsometry) spectroscopic ellipsometer. Values of $\Psi$ and $\Delta$ were obtained over the spectral range comprised between 300 and 1000 nm, at 5nm resolution. To check the consistency of the data, they were collected at three angles of incidence: 65º, 70º, and 75º. Optical modeling and parameters fitting were carried out with the WASE32© program (J.A. Woollam Co.,Inc.). To model the ellipsometric spectra we fixed the thickness (thickness values were obtained by transversal SEM images) and applied non-ideal model options such as film thickness non-uniformity and angular spread of the beam entering the detector. Some fitting parameters were coupled among them and their range limited within defined values. Non partial polarization or monochromator bandwidth effects were considered. Quality assessment of the fit data was performed by using the mean-squared error (MSE) value. A small MSE implies that the assumed model was appropriate. In our case, the MSE was below 5 units in the absorbing region and below 2 units in the transparent region. The used optical model consists of two layers deposited on the Si (1 mm) substrate: an external region and an EMA (effective medium approximation) layer with a harmonic oscillator. In this layer a Cauchy dispersion (with Urbach absorption)) and a classic harmonic oscillator model were implemented in a single material layer. The Cauchy dispersion equation was used in the transparent region ($\lambda$ > 700nm). No dispersion of

refractive index and in the extinction coefficient were considered for 700<λ< 1000nm. For λ < 700nm one or two harmonic oscillators were added to the Urbach absorption of the Cauchy model. Finally, a certain surface roughness consisting of 50% of film material and 50% of voids was assumed to describe the external layer.

XPS spectra of the films were recorded on an ESCALAB 210 spectrometer working under energy transmission constant conditions. The Mg Kα line was used for excitation of the spectra. They were calibrated in binding energy (BE) by referencing the different peaks to the C1s signal due to contamination taken at 284.6 eV. Quantification was done by calculating the area of the peaks and by correcting then with the sensitivity factor of each element/electronic level. To check the effect of surface impurities, the films were subjected to a gentle sputtering with $Ar^+$ ions of 2.5 keV. A current density of about 10 μA $cm^{-2}$ for a sputtering time of 2 min was used for these treatments. No significant changes in peak shape or in element ratio (except for the removal of most of the contaminating carbon) were found after this cleaning treatment. Fitting analysis of the N1s peak was carried out by using elemental bands of gaussian/lorentzian shape after background subtraction of the spectra with a Shirley-type curve.

SEM cross section and normal images were measured in a Hitachi S5200 field emission microscope for thin films grown on a silicon wafer.

Structural characterization of the thin films was done by X-ray Diffraction in a Siemens D5000 difractometer working in the Bragg-Brentano configuration and using the Cu Kα line as excitation source.

Measurement of the surface electrical conductivity of the samples was carried out with the typical four point probe test. A Keithley 617 Electrometer and a Hewlett-Packard 34401 A Voltammeter were used for the measurements. These consisted of applying a voltage ranging between -0.25 and 0.25 V to the two external probes and the measurement of the current flowing between the two internal probes.

Measurement of water contact angles was carried out by the Young method by dosing small droplets of deionized and bidistilled water on the surface of the illuminated samples. In the experiments where the contact angle variation was determined as a function of the illumination time, a metal foil acting as a shutter was used to close and open the lamp output. All wetting angle measurements within a given experiment were taken after illumination for successive periods of time. Therefore, the time scale in the plots refers to the accumulative illumination of the samples. The maximum uncertainty

in the determination of the water contact angle is about 10º depending on the sample position. In the course of this investigation it was noticed that the "as-prepared" thin films were more hydrophilic than the same samples some time after their preparation. Therefore, the reported results correspond to samples that were stored in desiccators for at least two months before testing their photo-activity. Illumination of the samples was carried out with a Xe discharge lamp with photon intensity at the position of the samples of 2 $Wcm^{-2}$ for the complete spectrum. For simplicity we will refer this situation in the text and figures as UV illumination. Other experiments consisted of the illumination with the same lamp by placing an UV filter (i.e., $\lambda > 400$ nm) between the lamp and the sample. The light intensity at the sample position was then 1.6 $Wcm^{-2}$. In all cases an infrared filter (i.e., a water bath) was kept between the lamp and the samples to prevent any possible heating by the infrared radiation.

*2.3 Computational details*

All the calculations were performed using the Vienna Ab-initio Simulation Package (VASP) 4.6 code,[36-38]. Inner core electrons were described by the projector-augmented-wave method[41] (PAW) and a 500 eV cut-off energy. The Ti (3s, 3p, 3d, 4s), O (2s, 2p) and N (2s, 2p) electrons were treated as valence states, while the remaining electrons were kept frozen as core states. The optimisation of the structures was performed via a conjugated gradient technique, which utilises the total energy and the Hellmann-Feynman forces on the atoms (and stresses on the unit cell). The Brillouin-zone integrations were performed using Monkhorst-Pack grids,[42] using a (2x2x1) mesh, with which convergence in energy was achieved. The simulation cell is formed by a 2×2×3 repetition of the anatase unit cell, in which there are 72 Ti atoms and 144 O atoms. We have employed a LDA+U approach, as described by Dudarev et al,[43-45] with a value of U of 4.5 eV. Calzado et al.[46] found that this value of U yields a correct description of the gap states in periodic LDA+U calculations. All calculations have been carried out in the Finis Terrae supercomputer, in Santiago de Compostela, Spain.

## 3. Results

### *3.1 State and concentration of nitrogen in N-$TiO_2$ thin films*

The amount of nitrogen incorporated in the film varied by changing the precursor and the plasma process parameters. Adjusting the plasma gas composition by using different $O_2$+$N_2$ mixtures as plasma gas was very important for this purpose. The OES spectra of the plasmas of these mixtures for $N_2$ concentration higher than 80% were characterized by a series of peaks and bands attributed to $N_2$* and $N_2^+$ species (see supporting information S1).[47,48] These nitrogen bands substitute those attributed to $O_2$* and O* that characterize the spectra recorded in our experimental system when pure oxygen is used as plasma gas.[27] A summary of the main species and spectral features detected as a function of the $O_2/N_2$ ratio are reported in the supporting information S1 and in a previous contribution of our group.[49] From this analysis it is important to realize that although nitrogen excited species detected by OES are majority in the $N_2/O_2$ plasmas, this does not necessarily preclude the formation of activated oxygen species, but just indicates that the average life time of these latter species are short as compared with that of the nitrogen species. The high reactivity of the oxygen species accounts for the formation of a titanium oxide film and enables the release of the carbon and hydrogen atoms of the precursors in the form of volatile oxidized compounds. Simultaneously, the presence of active species of nitrogen in the plasma provides a mechanism for the incorporation of nitrogen in the film by the reaction with the partially decomposed precursor molecules in the plasma phase or on the surface of the growing film. We will show later that the amount and type of incorporated nitrogen depends on the ratio between nitrogen and oxygen in the plasma gas.

Plasma deposition of $TiO_2$ thin films has been typically carried out by using TTIP as titanium precursor. The use of other precursors like TDMAT and TDEAT offers the possibility to incorporate some nitrogen within the structure even if no molecular nitrogen is added to the plasma gas, provided that some of the Ti-N bonds existing in the precursor molecules are preserved in the films. To verify this possibility we have analyzed by XPS a series of films prepared with a plasma of pure oxygen but using TTIP, TDMAT and TDEAT as precursors and 523 and 298 K as substrates temperatures. It was found that small amounts of nitrogen became incorporated in the films prepared with TDMAT and TDEAT precursors (see supporting information S2).

The incorporation was more favorable at 298 K. For all samples the O1s and Ti2p spectra were similar to those amply reported in the literature for $TiO_2$.[50] The N/Ti ratios deduced from the quantitative analysis of the spectra of the N-$TiO_2$ films prepared at 523 K and $O_2$ as the sole plasma gas were 0.037, 0.017 and 0.0 for the TDEAT, TDMAT and the TTIP precursors, respectively. The N1s spectra of the two former films were characterized by a broad peak at around 400 eV (see supporting information S2) which is commonly attributed to interstitial nitrogen species bonded to titanium and oxygen (i.e., a kind of Ti-N-O species[12, 22]). Similar spectra were obtained when the deposition was carried out with a substrate temperature of 298 K, although the intensity of the N1s signal was approximately twice higher in this case. It is also important to mention that the width of this N1s peak was also higher at 523 K (i.e., a HWHM of 2.8 eV) than at 298 K (i.e., a HWHM of 1.8 eV). This difference suggests that the nitrogen signal at 523 K is a convolution of different species of nitrogen. N1s spectra with more than one component at around 400 eV have been reported by several authors.[51-53] Their development in our case would indicate that at 523 K there are nitrogen species with slightly different geometries and bonding arrangements.

The concentration and type of nitrogen species in the N-$TiO_2$ thin films changed when mixtures $O_2$+$N_2$ were used as plasma gas. Under these conditions the main parameter controlling the incorporation of nitrogen into the films was the concentration of nitrogen in the gas mixture. Figure 2 shows a series of N1s spectra taken for films prepared at 523 K by using TDMAT as titanium precursor and increasing concentrations of $N_2$ in the plasma gas. Similar spectra were obtained for the other precursors. It is found that for percentages of $N_2$ higher than 85%, a new nitrogen species at around 396 eV appears in the spectrum. This species becomes dominant for higher percentages of nitrogen in the plasma gas. Similar results were obtained for the two other precursors, thus sustaining that the plasma gas composition and not the type of precursor is the main variable controlling the amount of nitrogen incorporated into these films. This new form of nitrogen has been attributed on the basis of XPS studies to nitride species in substitutional positions of the titanium oxide lattice (i.e., a Ti-N species[1, 7, 10 53-55]). The combined XPS, NEXAFS and Rietveld analysis made recently by H. Chen et al[55] for ammonia treated titania have quite unequivocally supported this attribution. It is also worthy of note that for most investigated films the shape of the O1s and Ti2p spectra is similar to that reported for $TiO_2$, thus indicating that the upmost surface layers of the

films have become oxidized by exposure to the air. Nevertheless, the shape of the Ti2p spectrum of the films prepared with a 97% of nitrogen in the plasma gas slightly changed with the development of a shoulder at lower binding energy, evidencing that some $Ti^{n+}$ species (n<4) remain in the surface of this sample even after its handling in air.

A deeper insight into these spectra can be obtained by fitting. Fig. 3 shows such an analysis for some selected case examples taken from Fig. 2 and others corresponding to thin films prepared with TTIP as precursor. The two sets of samples were synthesized with relative $N_2$ contents in the plasma gas of 0, 90 and 97%. In the case of the TDMAT samples, the spectra can be properly fitted with four bands located at 396.1, 399.3, 400.7 and 401.7 eV, the three latter accounting for the broad peak at around 400 eV. Meanwhile, a reasonable fitting could be obtained for the spectra of the TTIP samples by using just three bands at 396.1, 399.3 and 400.7 eV. A variety of peaks with N1s BEs comprised between 399 and 402 eV were already found in the early work of Saha et al.[56] dealing with the thermal oxidation of titanium nitride. Because of the similarities of the preparation techniques, it is also worth mentioning a recent publication by Chen et al.[26] where they investigated by XPS the type of nitrogen species incorporated into N-$TiO_2$ powder samples prepared by an atmospheric plasma procedure and posterior annealing. These authors found different components in the N1s photoelectron spectra, which they attributed to Ti-N (395.8-397.8 eV), Ti-NO (398.8-401.2 eV) and Ti-$NO_2$ (402.0-403.0 eV) species, in good agreement with our own results. Another relevant result of that work was the verification that the latter species was inactive in inducing any visible photo-catalytic activity. Similarly, Dunnill et al.,[57] using a thermal chemical vapor deposition process at 500 ºC for the preparation of N-$TiO_2$ thin films, found that in the majority of cases a peak at 400 eV was the only species detected and that these samples presented photocatalytic activity in the visible. Based on these and many other recent studies,[1, 7, 10, 12, 22, 51-55] we attribute the different features to Ti-N (i.e., band at 396.3 eV assigned to nitrogen triple bonded to titanium) and to nitrogen in a titanium oxinitride local environment (399.3 and 400.7 eV), where nitrogen simultaneously bonds to oxygen and to titanium in a defective lattice site (i.e., in a kind of Ti-N-O or Ti-O-N local structure). Meanwhile, the fourth band at 401.7 eV, observed in samples prepared with the TDMAT and TDEAT precursors, must be attributed to N bonded to a less electropositive environment or, alternatively, to a large

number of oxygen atoms. Therefore, we attribute tentatively this band to Ti-$NO_2$ species (i.e. a nitrogen atom bonding simultaneously to one titanium and two oxide ions of the lattice [26]). A similar attribution has been made recently by Asahi et al[53] based on first principles calculations for a peak with a BE higher than that of the band used here for fitting. For simplicity, in the rest of the paper we will refer to Ti-N and Ti-NO species (this latter including the species that we have designed as Ti-ON), even if different environments, and therefore BEs, can be expected for the different interstitial species of nitrogen. Theoretical calculations have been performed for Ti-N (i.e., $N_s$ according to the notation used with the calculations with the model systems), Ti-NO (i.e. $N_i$) and Ti-ON (i.e. $N_{si}$) species in *section 3.3*.

XPS has been also used to quantitatively estimate the concentration of nitrogen in the films as a function of the plasma deposition conditions. Figure 4 shows a plot of the N/Ti ratio as a function of the relative concentration of nitrogen in the plasma gas determined by XPS for an ample series of thin films prepared at 523 K. In this plot we make no distinction according to the precursor used for their synthesis, as the plasma gas composition is the main parameter controlling the nitrogen content. It is also important to mention that at 298 K the amount of incorporated nitrogen was always slightly higher than at 523 K for $N_2/O_2$ ratios higher than 50% (data not shown). The plot in Fig. 4 shows that the concentration of nitrogen in the film remains relatively constant up to $N_2$ percentages of 80-85%. Above these values, the concentration of nitrogen in the films sharply increases, reaching N/Ti ratios of ca. 0.5 when a 97% nitrogen plasma was used for the synthesis. As mentioned previously, for this sample the shape of the Ti2p spectrum broadens towards lower BEs, pointing to certain reduction of the titanium cations and the formation of oxygen vacancies within the lattice. The incorporation of nitrogen, particularly in the form of Ti-N species, and its relationship with the formation/elimination of oxide vacancies within the lattice has been addressed previously in the literature both experimentally and theoretically. [25, 34, 54, 55] In relation with these previous works dealing with an already formed $TiO_2$ network where nitrogen is added either by ion implantation or upon annealing in ammonia, our experimental conditions are different because the N-$TiO_2$ materials are created directly by the deposition and/or reaction of/with plasma species. However, the fact that the maximum concentration of Ti-N species appears when the oxide is defective suggests

that the incorporation of this nitrogen species becomes favored in partially reduced titanium oxide networks.

*3.2 Optical and electrical properties of N-doped titanium oxide films*

The progressive incorporation of nitrogen into the films, particularly in the form of Ti-N species, induces significant changes in their optical behavior. Fig. 5 shows a series of UV-vis absorption spectra recorded for selected thin films prepared with TDMAT as precursor and 85%, 90%, 95% and 97% $N_2$ in the plasma gas. It is important to note that the three latter samples, have incorporated a considerable amount of nitrogen (cf. Figs. 3 and 4). These spectra are compared with the spectrum of a film prepared with 0% $N_2$ taken as a reference. All the curves are characterized by the typical oscillatory behavior found when a high refraction index (**n**) material is deposited on a transparent substrate with smaller **n.** These oscillations are originated by the interference of the partially reflected beams at the film/air and film/substrate interfaces.[58] Besides these oscillations, another quite remarkable effect is the shift of the absorption threshold to lower wavelengths for thin films prepared with percentages of nitrogen higher than 85%. Usually, this shift has been recognized in the literature as a hint of visible photo-activity in doped $TiO_2$, [17-20] although this correlation has been claimed as a necessary but not sufficient condition.[22-24, 59] It is also important to remark in this figure that the minima of the oscillations recorded for the sample prepared with 97% $N_2$ appear quite above the curve of the reference $TiO_2$, which indicates a significant absorption in the visible region (i.e., for $\lambda$>500 nm). For percentages of $N_2$ in the plasma smaller than 85%, for which the amount of incorporated nitrogen is still small (c.f. Fig.s 3 and 4), the shape of the curves, except for the oscillatory behavior in the transparent region that depends on the film thickness, was similar to that corresponding to the film prepared with 0% $N_2$ and did not depict any clear hint of a shifted absorption edge. Similar sets of curves were obtained when using either TTIP or TDEAT as titanium precursor. For the whole set of investigated samples, we have calculated the value of the absorption threshold by assuming a Tauc model for the evaluation of the band gap of $TiO_2$ (i.e., $A(h\nu)^{1/2}$).[60] The obtained values are represented in Fig. 6. The shape of the curve defined by the different points is the reverse to that in Fig. 5, corresponding to the relative concentration of nitrogen incorporated into the films. Consequently, a representation of the absorption threshold values against the N/Ti ratio in the films follows a linear tendency (see supporting information S3). This behavior indicates that the absorption

threshold of the N-$TiO_2$ films is controlled by the amount and perhaps the type of incorporated nitrogen. For the samples prepared with $N_2$ percentages higher than 85% the Ti-N species, incorporated then in a substantial amount, is the most abundant species, as evidenced by the shape of the XPS spectra in Figs. 2 and 3. These samples present a clear shift in the absorption threshold whose magnitude is correlated with the amount of nitrogen within the lattice (cf. Figs. 5 and 6). By contrast, samples prepared with 85% or a lesser amount of nitrogen in the plasma, incorporate a limited amount of nitrogen in the form of Ti-NO species. These samples do not present a clear shift in the absorption threshold, although a clear determination is difficult with absorption spectra such as those in Fig. 5, where the presence of interference oscillations may mask changes at the edge spectral region.

Electrical characterization of the films prepared with a high concentration of $N_2$ in the plasma gas showed that they present a certain sheet conductivity (see supported information S4) which is indicative of some reduction of the titanium ions and the presence of a certain concentration of oxygen vacancies within the lattice.[61] The broad absorption feature extending through all the visible region of the spectra (i.e., $\lambda$>500 nm) found for the samples prepared with 97% $N_2$ can therefore be associated with the lost of stoichiometry in these samples.[21] This confirms our evidences based on the analysis of the Ti2p XPS spectra and supports the already commented relationship between the incorporation of Ti-N species and the formation of oxygen vacancies within the lattice. [25, 34, 54, 55]

Owing to the oscillatory behavior of the UV-visible transmission spectra, it is difficult to ascertain if real absorption features close to the absorption threshold superimpose in the spectra of the films prepared with percentages of $N_2$ lower or equal than 85%, where only Ti-NO species have been determined by XPS. In order to check this point, we employed ellipsometry to determine the extinction coefficient (**k**) and refraction index (**n**) functions of selected films for $\lambda$> 300 nm. The corresponding plots are shown in Fig. 7 for three thin films prepared at 523 K with TDMAT as precursor and percentages of $N_2$ in the plasma gas of 0%, 85% and 97%. For the whole spectral region, the refraction indices of the 97% $N_2$ film was higher than those of the other two samples (e.g., at $\lambda$=550 nm, the measured values were 2.38 and 2.12, respectively), in agreement with its UV-vis absorption spectrum (Fig. 5) and its extinction coefficient curve plotted in the bottom panel of Fig.6. This latter curve is characterized by a broad and intense

maximum at around 400 nm that defines a shifted absorption threshold of 2.11 eV, extending to cover the whole visible region of the spectrum. By contrast, the extinction coefficient curve of the film prepared with 85% nitrogen does not present this broad absorption and its edge jump defines an absorption threshold of 3.19 eV, quite similar to that of the film prepared with pure oxygen as plasma gas. The main difference between the curves of the samples prepared with 0% and 85% $N_2$ consists of a small but well defined absorption feature at around 375 nm in the extinction coefficient curve of the latter (indicated by a star in the figure). An absorption feature in this position was indeed needed to extract a reasonable extinction coefficient curve from the ellipsometric data recorded for this film.

### *3.3. Density of states calculations for model N-TiO2 systems*

The three model systems used to calculate the density of states of the different N-$TiO_2$ thin films are shown in Fig. 8. They represent the substitutional, $N_s$ , interstitial, $N_i$ and substitutional-interstital, $N_{si}$ defect states. In this latter type of defect state, N occupies the same position as in the case of the $N_s$ defect, but there is also an O atom occupying an interstitial site. We will assume that these states of nitrogen correspond to the XPS bands attributed in section 3.1, namely Ti-N, Ti-NO and Ti-ON species. Calculations based on structures similar to those of the two former types of defects have been previously carried out by Di Valentin et al [12,13, 15] to account for modifications of the band structure in N-doped $TiO_2$. These authors have also considered either the effect of Ti-N[12,13, 15] or Ti-NO[12, 13] like species, although they employed smaller simulation cells (with 96 and 72 atoms for the anatase and rutile supercells respectively). Herein, besides studying the effect of another type of species (i.e., Ti-ON), we address systematically the possible influence in the electronic structure of the concentration of incorporated nitrogen for both the Ti-N and Ti-NO species in a larger supercell, with 216 atoms. To simulate the influence of the concentration of nitrogen in real samples, we have considered two different simulation cells for each system, one containing one defect, and another containing two defects. In addition, in this latter case we have used two different arrangements for the two defect states, placing them in either two nearby or in quite separated positions within the lattice. These two geometries are employed to represent the electronic structure of N-$TiO_2$ systems with, respectively, a high and a low

concentration of nitrogen. The most relevant geometrical parameters of the studied defect configurations are reported in Table 1.

We also performed calculations on a different type of defect, in which the O atom was initially placed at its equilibrium lattice location, and the N atom is in an interstitial site above the O atom at a distance of 1.35 Å along the z axis. We studied two systems with one and two defects of this kind. Upon the energy minimization, the cells underwent large geometrical rearrangements leading in the two cases to final configurations equivalent to that of the $N_i$ defects. This suggests that this initial configuration is not stable and that minimization of the energy is accomplished by a displacement of the O atoms from their initial location and their substitution by nitrogen. This also means that the assumed detection by XPS of these species in some of our samples (i.e., band at 401.7 eV of BE, cf. Fig. 3) is likely related with the fact that the plasma deposition process utilized for the synthesis of the N-$TiO_2$ films is an out of equilibrium procedure.

The calculations also provided interesting information regarding the energy of the different studied systems. Thus, when $TiO_2$ is modified with $N_S$ defects, the energy of the system where the two defect states are in nearby positions is 29.1 kJ/mol higher than the energy of the system in which the two defects are far away. When considering $N_i$ defects, this energy difference is much smaller, just -1.1 kJ/mol, which means that there is no strong energetic driving force preventing the aggregation of $N_i$ defects. In the case of $N_{Si}$ defects, this energy difference is 14.0 kJ/mol, indicating that it is energetically favourable to keep $N_{Si}$ defects as far away as possible within the lattice. On the other hand, to determine the relative stability of the $N_{Si}$ and $N_i$ defect states we can compare directly the energies of the corresponding systems, as they have the same number of atoms. For the systems modelling low nitrogen concentrations (with defects far away from each other), we find that $N_i$ defects are 8.3 kJ/mol more stable than $N_{Si}$ defects. Meanwhile, for the systems modelling a high concentration of nitrogen, the $N_i$ defects are 29.0 kJ/mol more stable than $N_{Si}$ defects, a result which suggests that $TiO_2$ materials with a high concentration of nitrogen will tend to have $N_S$ and $N_i$ defects and that the formation of $N_{Si}$ defects would not be favoured.

The total densities of states (DOS) calculations for pure $TiO_2$ (shown in the Supporting Information S6) predict a gap between the valence and conduction bands of

2.7 eV. This value is smaller than the experimental band gap of anatase $TiO_2$ (i.e., 3.2 eV[62]), a difference that is due to the well known underestimation of the band gap in DFT calculations.[63] The value of the Hubbard parameter U that we used is 4.5 eV, which provides a good description of the gap states in periodic LDA+U calculations of $TiO_2$ and, at the same time, predicts a reasonably good value for the band gap (i.e., 2.7 eV).[46] A similar result has been also obtained by Di Valentin et al.[11] when modeling N-$TiO_2$ systems.

The total densities of states (DOS) of the six N-$TiO_2$ studied systems are shown in Fig. 9. The reported results indicate that the N-$TiO_2$ systems have developed new electronic states in the band gap close to the valence states of titanium dioxide. A similar result has been obtained by other authors simulating the electronic structure of N-$TiO_2$ systems, [11-15, 25, 34] although in these previous works smaller supercells were employed in the calculations. Particularly interesting with regard to the optical properties of N-$TiO_2$ is the difference observed in Fig. 9 between the shape of the gap states corresponding to the $N_s$ and the $N_i$ and $N_{si}$ defects around the HOMO level (marked with a continuous line in the figure). In the former case (i.e. DOS curves a) and b)) the extra states due to the incorporation of N appear as a continuous prolongation of the valence band states of pure $TiO_2$ (marked with a dashed line in the figure). By contrast for the case of $N_i$ and $N_{si}$ defect states, the N-related gap states appear as well defined discrete peaks separated from the valence band of $TiO_2$ (i.e. DOS curves c)-f)). Phenomenologically, this difference is equivalent to say that the $N_s$ defects have induced a shift of the valence band edge, producing a decrease in the gap of the system, while the $N_s$ and $N_{si}$ states do not modify the valence band of $TiO_2$ but introduce new electronic states in the gap. This point has been previously discussed based on both experimental[54] and theoretical[11-15] studies. Thus, Diebold et al.[54] studied by XPS and valence band photoemission N-implanted anatase and rutile, and concluded that localized states rather than a band gap narrowing develop upon nitrogen implantation and the subsequent formation of $N^{3-}$ (i.e., Ti-N) species. Theoretically, studying the anatase polymorph, Di Valentin et al[11-12] concluded that substitutional nitrogen states (i.e., Ti-N) lie just above the valence band, while interstitial nitrogen states (i.e., Ti-NO) lie higher in the gap. These authors also found that Ti-N species in rutile might produce a certain increase of the gap with the N-associated states close to the valence band maximum.[15] The main difference between these previous studies and our calculations

reside in the fact that we deal with more than one nitrogen species and define two different scenarios for them depending on whether they are located in separated or close positions of the lattice. When N atoms are close, as in the DOS curves a), c) and e), the number of gap states is higher and appear more scattered along the band gap, as if there is a splitting of peaks due to the electronic interaction between defects. By contrast, when the N atoms are separated within the lattice, as in DOS curves b), d) and f), there is a smaller number of peaks in the gap and they tend to be more concentrated around certain energy values in the band gap (i.e., more localized states). In particular, for the $N_s$ species located in nearby lattice positions, it appears that the $TiO_2$ valence band maximum extends continuously to higher energies. From an experimental point of view, this is equivalent to say that there has been a narrowing of the gap. This would be in fact the situation for our samples prepared with nitrogen percentages in the plasma higher than 85% (cf. Figs. 4 and 5).

As shown in the partial density of state plots in Fig. 10, the new states developed in the gap have a mixed titanium-nitrogen-oxygen character and show slightly different features depending on the kind of nitrogen defect considered in each case. This figure represents in an enlarged scale the gap zone to clearly depict the new states appearing in the N-$TiO_2$ systems. The plots represent the titanium, oxygen and nitrogen projected states of the DOS curves in the regions around the HOMO lines in each system (note that the HOMO lines appear at different energies in each case). For oxygen, they are represented both the states corresponding to the oxygen atoms close to nitrogen and those located in separated positions. This distinction is important since for the $N_i$ and $N_{si}$ states nitrogen is directly bonded to an oxygen atom whose contribution to the DOS of the new states is expected to be quite substantial. The first conclusion we could draw from these plots is that all the defect states have a mixed character with contributions from the oxygen, nitrogen and titanium atoms. However, a closer look to these curves also reveals that in the $N_s$ defects the nitrogen contribution to the gap states is relatively higher than that of the close oxygen atoms, while for the $N_i$ and $N_{si}$ defects the nitrogen and close-oxygen contributions are rather similar, thus supporting the importance of these oxygen atoms in determining the electronic properties of the system. This closer look to the new states around the HOMO line also suggests that the DOS curves of the $N_s$ defects, particularly for the case with the two nitrogen atoms located in nearby positions, are a continuous extension of the valence band. The fact that the nitrogen

contribution to these states extends through the entire DOS region, both bellow and above the HOMO line, supports our view in the sense that a narrowing of the valence band has occurred in this case. By contrast, for the $N_i$ and $N_{si}$ defects, the nitrogen contribution to the new states appears quite concentrated in localized levels that do not form a continuum with the valence band states. This result suggests that even for N-$TiO_2$ systems with a high concentration of Ti-NO species, their electronic structure can be described by the appearance of localized states in the gap.

*3.4 Wetting angle photo-activity of N-TiO2 thin films*

The photo-activity of N-$TiO_2$ thin films has been the subject of a large debate during the last years.[1-14] In recent publications we have shown that transformation of the surface state of N-$TiO_2$ from partially hydrophobic (i.e., wetting contact angles around 80º) into hydrophilic can be induced by visible light in samples containing Ti-NO species, regardless of whether they were amorphous or crystalline. By contrast, visible photo-catalytic activity towards, for example, the photo-degradation of dyes seems to constitute a more demanding process, which requires titanium oxide to be in crystalline phase, forming a mixture composed mainly by anatase and a small amount of rutile.[22]

In agreement with previous studies with PECVD $TiO_2$ thin films using TTIP as volatile precursor of titanium and pure oxygen as plasma gas[25]), we have found that amorphous $TiO_2$ is obtained for deposition temperatures lower than 523 K and that the anatase phase of this oxide is obtained for $T \geq 523$ K. By contrast, most N-$TiO_2$ thin films prepared at this temperature with TDMAT and TDEAT as precursors were amorphous, as shown by their XRD spectra (see supporting information S7). Since no photo-catalytic activity was found for any of the N-$TiO_2$ thin films when illuminated with visible light and very little when using UV light, to check the possible role of the different nitrogen species in controlling the visible photo-activity of these materials we have looked for changes in wetting contact angle under visible and UV light illumination. Fig. 11 presents some selected results showing that for samples containing Ti-NO species (i.e., a sample prepared with 85% $N_2$) the wetting angle decreases by almost 50º when illuminated with visible light, while for the films with a high concentration of Ti-N species (i.e. sample prepared with 97% $N_2$ ) no visible light effect was observed. This different behavior according to the type of nitrogen species was common for the rest of N-$TiO_2$ thin films. When after the visible illumination the

samples were irradiated with UV light, we found that all of them became superhydrophilic (i.e., wetting angle lower than 10º), which is the typical behavior of UV-illuminated $TiO_2$ thin films. Even if wetting induced changes and photo-catalytic processes are not equivalent tests of $TiO_2$ photo-activity,[22, 64] the reported results in Fig. 11 clearly prove that Ti-N species are unable to induce visible light photo-activity and that the presence of Ti-NO species in the films is a requisite for promoting visible light activation of N-$TiO_2$ thin films, at least for a partial hydrophilic conversion of their surface.

## 4. Discussion

The previous results on N-$TiO_2$ thin films prepared by PECVD have provided information about both the influence of the incorporated nitrogen on the optical properties of $TiO_2$ and on the characteristics of the nitrogen species incorporated within the structure of the oxide according to the different conditions of preparation. In relation with this latter aspect, we have also described theoretically how the different species of nitrogen may affect the electronic structure of the prepared materials. The influence of these species of nitrogen on the photo-activity of N-$TiO_2$ is finally discussed in relation with visible-light hydrophilic conversion of the surface of the prepared films.

### *4.1.-Type and concentration of nitrogen species and band gap narrowing in N-$TiO_2$ thin films*

The previous XPS results have shown that the incorporation of small amounts of nitrogen in the form of Ti-NO species (i.e., $N_i$ defects according to the notation used for the density of states calculations) occurs when using TDMAT or TDEAT as precursors or when the films are deposited with a $O_2$+$N_2$ plasma mixture with less than 90% of nitrogen. We have proposed that the existence of four Ti-N bonds in the two latter precursor molecules may account for the presence of Ti-NO species in these films, even if no nitrogen gas has been added to the plasma. For 90% or higher concentration of nitrogen a progressive incorporation of Ti-N species takes place. For all experimental conditions used for the synthesis of the N-$TiO_2$ films we have also found that the amount of incorporated nitrogen species (Ti-N and Ti-NO) was higher at low (i.e., 298 K) than at high (523 K) temperatures. The stability of Ti-N implanted in rutile and

anatase polymorphs of $TiO_2$ has been addressed in previous articles,[34, 54] where a certain desorption upon annealing has been observed only for the case of anatase[54] and an extra stabilization is achieved when gold is deposited onto the surface.[34] These results have been interpreted in terms of the interaction of the implanted nitrogen (and deposited gold particles) with oxygen vacancies in the lattice.[25,34, 54] Although most of our films were amorphous and a comparison with literature data is therefore not straightforward, we must stress that our results point to a certain relationship between the formation of Ti-N species and the existence of oxygen vacancies within the lattice. The aforementioned dependence of the Ti-N concentration on the temperature of the PECVD process and the fact that the maximum concentration of this species is found for defective and high conductive samples support such dependence.

Ti-N and Ti-NO species of nitrogen have been previously detected and discussed in literature,[1, 12, 22, 51-57] although no complete agreement exists on their specific role in altering the electronic and optical properties of N-$TiO_2$ materials. In fact, during the last years there has been a vivid discussion on whether modifying the $TiO_2$ with nitrogen produces a shift in the absorption edge or just the development of absorption centers close to an unmodified gap. Our experimental results indicate that both localized band states and band gap narrowing may occur depending on the type and concentration of nitrogen species incorporated within the films. Thus, we have found experimentally that the incorporation of a relatively low concentration of interstitial nitrogen (i.e. Ti-NO species) does not modify substantially the band gap structure of the oxide, but induces the formation of some localized electronic states in the gap (cf. Figs. 5 and 7). A similar situation has been claimed in the theoretical works of Di Valentin et al.[11-15] By contrast, our data suggest that a narrowing of the band gap due to a shift in the valence band edge may occur when substitutional nitrogen (i.e. Ti-N species) is incorporated within the lattice. We have also found that the magnitude of this shift is directly related with the amount of incorporated Ti-N species that we control by changing the relative amount of nitrogen in the plasma. In recent experimental [54] and theoretical[11-15] studies on titanium oxide with incorporated Ti-N species such a narrowing has not been detected, a difference that might be related with the fact that in these experiments a lower concentration of nitrogen species was actually incorporated within the lattice and because only the effect of isolated nitrogen species was theoretically modeled.

The films with a high concentration of nitrogen in the form of Ti-N species (i.e., those prepared with a $N_2$ percentage of 95% or above) present a loss in transmission that has been associated with the formation of oxygen vacancies (associated with $Ti^{n+}$ species, n<4, detected by XPS) that would be responsible for a wide absorption extending over a large zone of the visible spectrum.[21, 61] The decrease in the resistivity of these films (cf. supporting information S7) confirms that these films are oxygen defective, again suggesting that incorporation of Ti-N species becomes favored by the presence of oxygen vacancies. [25, 34, 54]

*4.2. Density of states and electronic structure in N-$TiO_2$*

The density of states calculations reported in *section 3.4* account for the different phenomenological behaviors found for N-$TiO_2$ thin films depending on the type and concentration of the nitrogen species incorporated into the lattice. We have shown that the $N_i$ and $N_{si}$ defects, associated to the Ti-NO and Ti-ON species detected by XPS, give rise to localized electronic states in the gap above the valence band edge of the oxide. In previous works, Di Valentin et al[11,13, 15] reached a similar conclusion by simulating the electronic structure of isolated $N_i$ defect states. We have investigated the influence of inter-defect distances on the electronic properties, in larger supercells. For a two-defect model simulating the incorporation of a high concentration of $N_i$ species within the lattice (cf. Figs. 9 and 10), we have also proved that the gap states do not become extensively mixed with the valence band levels of the oxide and keep a localized character. This theoretical result supports the experimental findings by ellipsometry and UV-vis spectroscopy for the 85% $N_2$ sample (cf. Fig. 7), where the presence of a localized harmonic oscillator at around 375 nm is required for a good fitting of the experimental curves. Unfortunately, our experimental protocol does not enable the incorporation of a high concentration of Ti-NO species without Ti-N species being also formed. This limitation might be explained by the calculated energies of formation of the different defect states (*section 3.4*). Even though, the good agreement between experimental and theoretical results supports the development of isolated states in the gap rather than a band gap narrowing in the samples prepared with 85% or a lower concentration of $N_2$ in the plasma gas.

A direct comparison between our experimental and theoretical results is possible when dealing with the $N_s$ defect states (i.e., Ti-N species according to the notation used by the

XPS analysis) where, particularly for the structures simulating a high concentration of this species, a substantial mixing between the valence band states and those pertaining to the nitrogen can be deduced from the calculated partial density of state curves (c.f. Fig.10). As an overall effect, it can be interpreted that this mixing produces a shift towards the visible of the valence band edge, in agreement with our experimental observations for the samples prepared with nitrogen rich plasmas. As discussed in *section 4.1*, the different interpretation regarding the modifications of the gap that was outlined in previous theoretical[11-15] and experimental[54] works, might be connected with the fact that they simulate or interpret experiments with more separated Ti-N species. In this way, our description of the optical and electronic properties of N-$TiO_2$ systems with a high concentration of Ti-N species would be in a better agreement with the original suggestions of Asahi et al.[1] of a band gap narrowing than with those of these more recent works.

### *4.3. Wetting photo-activity of N-doped $TiO_2$*

Visible photo-activity of N-doped $TiO_2$ thin films is a very elusive effect with somehow contradictory results in the literature, where the red-shift of the valence band edge has been taken sometimes as a sufficient evidence warranting reactivity under visible illumination.[16] In recent works, it has been pointed out that although visible absorption is a required condition, it is not sufficient to assure visible photo-activity of N-$TiO_2$. Moreover, different conditions seem to be required for photo-catalysis and for light-induced wetting angle changes over flat surfaces of this material.[64] The former is a much more demanding process that, besides the presence of nitrogen species, requires that the nitrogen modified titania is crystalline and complies with some additional structural conditions, such as the simultaneous presence of both anatase and rutile polymorphs in the photo-active material.[22] Since most N-$TiO_2$ thin films prepared in the present work were amorphous, we have investigated the effectiveness of either Ti-N or Ti-NO species in inducing some kind of visible photo-activity by following the changes in wetting angle upon illumination with visible light. The experiments carried out with the N-$TiO_2$ thin films have shown that samples with a high concentration of Ti-N species do not show visible photo-activity and keep their original wetting angle even after a prolonged illumination with visible photons (cf. Fig. 11). By contrast, films containing Ti-NO species do present some visible photo-activity, which was evidenced by a partial and progressive decrease in the water contact angle of ca. 50º from an

original wetting angle of 98º to a wetting angle of 52 º after 60 min illumination. This behavior, even if occurring with a slow rate, indicates that in the presence of this species visible light is capable of photo-activating the surface of these titanium oxide samples. A thorough discussion of this kind of partial hydrophilic transformation of N-$TiO_2$ surfaces upon visible light irradiation can be found in reference 24.

Our theoretical and experimental results have shown that a small concentration of Ti-NO species in the films do not modify significantly the band gap of the oxide but induces some localized electronic states close to the band edge. Visible light excitation up to the conduction band of the electrons associated to these electronic states in the gap should render a conduction band electron and a localized hole in the gap state. We believe that precisely the localized character of this photo-hole is the factor precluding a continuous operation of these films as a photo-catalyst as the mobility of these photo-holes induced with visible light is rather limited.[15] Indeed, for a continuous photo-catalytic process to take place it is required the migration of both electrons and holes towards the surface, as it usually happens in undoped $TiO_2$ illuminated with UV light. In N-$TiO_2$ systems, migration towards the surface of the photo-holes generated in the illuminated layer (i.e. in the order of the micron) can only take place if a continuous band-like state forms in the gap. This is not certainly the case in our samples with a low concentration of incorporated Ti-NO species. However, as previously discussed by us,[24] visible-light partial conversion of the surface hydrophilicity occurs by just activating the utmost atomic layers whereby only surface electron-hole pairs are involved in the transformation. Therefore, the point to be stressed here is that while Ti-NO species are able to induce this visible-light transformation, Ti-N species aren't. This finding contrasts with the original proposal of Asahi et al.[1] and thereafter of other authors [5, 16] attributing to the Ti-N species the visible photo-activity of N-$TiO_2$ materials. However, it complies with more recent results stressing that for visible photo-activity to occur, Ti-NO like species must be present. [26, 56]

## 5.-Conclusions

The previous results have shown that by using the PECVD technique it is possible to obtain a large set of N-$TiO_2$ thin films where the amount and type of nitrogen can be tuned by controlling the working parameters during the deposition of the films. Thus, Ti-NO species are the only type of incorporated nitrogen species when the films were

prepared with a relatively low concentration of nitrogen in the plasma gas. On the other hand, a high concentration of Ti-N species becomes incorporated into the films for nitrogen rich plasmas.

Density of states calculations of differently doped anatase model systems have provided a detailed description of the influence of the N states, Ti-N and Ti-NO (and the related one Ti-ON), on the electronic structure of N-$TiO_2$. It is found that in anatase with a relatively high concentration of Ti-N species the valence band edge shifts upwards because of the mixing of the N atomic levels with the levels of the lattice atoms. Consequently, the absorption edge of the UV-vis absorption spectra is red shifted as found experimentally. On the contrary, for the Ti-NO species the electronic levels of the interstitial nitrogen species remain localized and no band gap narrowing occurs. Experimentally, this situation yields spectra whose absorption edge are not shifted but present a separated absorption oscillator close to it.

Films containing Ti-N species are not photo-active with visible light even if they present a red-shifted absorption edge. Visible light wetting photo-activity is only observed in N-$TiO_2$ films with Ti-NO defect states. This observation has been related with the surface excitation of the electronic states associated to these species, which appear in the gap close to a virtually un-modified valence band edge.

**6.-Acknowlegdments.-** We thank the Ministry of Science and Education of Spain (projects MAT 2007-65764 and the CONSOLIDER INGENIO 2010-CSD2008-00023) and the Junta de Andalucía (projects TEP2275/P09-TEP-5283/CTS-5189) for financial support. This work has been carried out within the EU project NATAMA (contract no. 032583)

**Supporting Information Available.**

Some additional information referred in the text as S1-S8 is available free of charge via the Internet at http://pubs.acs.org.

**References**

1.- Asahi, R.; Morikawa, T.; Ohwaki, T.; Aoki, K.; Taga, Y., Science **2001**, 293, 269.

2.- Diwald, O.; Thompson, T. L.; Zubkov, T.; Goralski, E. G.; Walck, S.D.; Yates, J.T., *J. Phys. Chem. B,* **2004**, 108, 6004.

3.- Nakano, Y.; Morikawa, T.; Ohwaki, T.; Taga, Y., *Appl. Phys. Lett.* **2005**, 86, 132104

4.- Diwald, O.; Thompson, T.L.; Goralski, E.G.; Walck, S.D.; Yates, J.T., *J. Phys. Chem. B* **2004**, 108, 52.

5.- Yates, H.M.; Nolan, M.G.; Sheel, D.W.; Pemble, M.E., *J. Photochem. Photobiol. A: Chemistry* **2006**, 179, 223.

6.- Thompson, T.L.; Yates, J.T., *Chem. Rev.* **2006**, 106, 4428.

7.- Emeline, A.V.; Kuznetsov, V.N.; Rybchuk, V.K.; Serpone, N., *Int. J. Photoener.* **2008** Art. ID 258394

8.- Mitoraj, D.; Kisch, H., *Angew. Chem. Int. Ed.* **2008**, 47, 9975.

9.- Trenczek-Zajac, A.; Kowalski, K.; Zakrzewska, K.; Radecka, M., *Mater. Res. Bull.* **2009**, 44, 1547.

10.- Oropeza, F.E.; Harmer, J.; Egdell, R.G.; Palgrave, R.G., *Phys. Chem. Phys.* **2010**, 12, 960.

11.- Di Valentin, C.; Pacchioni, G.; Selloni, A.; Livraghi, S.; Giamello, E., *J. Phys. Chem. B* **2005**, 109, 11414.

12.- Livraghi, S.; Paganini, M.C.; Giamello, E.; Selloni, A.; Di Valentin, C.; Pacchioni, G., *J. Am. Chem. Soc.* **2006**, 128, 15666.

13.- Di Valentin, C.; Finazzi, E.; Pacchioni, G.; Selloni, A.; Livraghi, S.; Paganini, M.C.; Giamello, E., *Chem. Phys.* **2007**, 339, 44.

14.- Napoli, F.; Chiesa, M.; Livraghi, S.; Giamello, E.; Agnoli, S.; Granozzi, G.; Pacchioni, G.; Di Valentin, C., *Chem. Phys. Lett*. **2009**, 477, 135

15.-Di Valentin, C. ; Pacchioni, G. ; Selloni A., *Phys. Rev. B* **2004**, 70, 085116

16.- Chen, X.; Burda, C., *J. Phys. Chem. B*, **2004**, 108, 15446

17.- Vyacheslav, N.; Kuznetsov, N.; Serpone, N., *J. Phys. Chem. B* **2006**, 110, 25203.

18.- Lei, Z.; Ma, G.; Liu, M.; You, W.; Yan, H.; Wu, G.; Takata, T.; Hara, M.; Domen, K.; Li, C.*; J. Catal.* **2006**, 237, 322

19.- Umebayashi, T.; Yamaki, T.; Itoh, H.; Asai, K., *Appl. Phys. Lett.* **2002**, 81, 554.

20.- Liu, B.; Wen, L.; Zhao, X. Solar Energy Mater.&Solar cells **2008**, 92, 1

21.- lin, Z.; Orlov, A.; Lambert, R.M.; Payne, M.C., *J. Phys. Chem. B*, **2005**, 109, 20948

22.- Romero-Gómez, P.; Rico, V.; Borrás, A.; Barranco, A.; Espinós, J.P.; Cotrino, J.; González-Elipe, A.R., *J. Phys. Chem. C* **2009**, 113, 13341.

23.- Nakamura, R.; Tanaka, T.; Nakato, Y., *J. Phys. Chem. B* **2004**, 108, 10617

24.- Borrás, A.; López, C.; Rico, V.; Gracia, F.; González-Elipe, A.R.; Richter, E.; Battiston, G.; Gerbasi, R.; McSporran, N.; Sauthier, G.; Gyorgy, E.; Figueras, A., *J. Phys. Chem. C* **2007**, 111, 1801.

25.-Graciani, J.; Alvarez, L.J.; Rodríguez, J.A.; Fernández-Sanz, J., *J. Phys. Chem. C* 2008, 112, 2624

26.-Chen, C.; Bai, H.; Chang, Ch., *J. Phys. Chem. C* **2007**, 111, 15228

27.- Borrás, A.; Cotrino, J.; González-Elipe, A. R., *J. Electrochem. Soc.,* **2007**, 154, 152

28.- Gracia, F.; Holgado, J.P.; González-Elipe, A.R., *Langmuir* **2004**, 20, 1688.

29.- Ahn, K.-H.; Park, Y.-B.; Park, D.-W., *Surf. Coat. Technol*. **2003,** 171, 198

30.- Nakamura, M.; Kato, S.; Aoki, T.; Sirghi, L.; Hatanaka, Y. *Thin Sol. Films* **2001**, 401, 138

31.- Song, XM,; Gopireddy, G.; Takoudis, C.G., *Thin Sold Films* **2008**, 516, 6330

32.- Song, XM; Takoudis, C.G., *J. Vac. Sci. Technol. A* **2007**, 25, 360

33.- Xie, Q.; Yiang, Y.L.; Detavernier, C.; Deduytsche, D.; Van Meirhaeghe, R.L.; Ru, G.P.; Li, B.Z.; Qu, X.P., *J. Appl. Phys.* **2007,** 102, art. N. 083521

34.- Graciani, J.; Nambu, A.; Evans, J.; Rodriguez, J.A.; Fernández-Sanz, J., *J. Am. Chem. Soc*. **2008**, 130, 12056

35.-Barranco, A.; Cotrino, J.; Yubero, F.; Espinós, J.P.; Clerc, C.; Gonzalez-Elipe, A.R., *Thin Solid Films* **2001,** *401*, 150

36.- Kresse G.; Hafner, J. *Physical Review B*, **1993**, 47, 558-561.

37.- Kresse G.; Furthmuller, J. *Physical Review B*, **1996**, 54, 11169-11186.

38.- Kresse G.; Furthmuller, J. *Comput. Mater. Sci.*, **1996**, 6, 15-50.

39.- Wang Y.; Perdew, J. P. *Phys. Rev. B*, **1991**, 44, 298.

40.- Perdew, J. P.; Chevary, J. A.; Vosko, S. H.; Jackson, K. A.; Pederson, M. R.; Singh, D. J.; Fiolhais, C. *Physical Review B*, **1992**, 46, 6671.

41.- Kresse G.; Joubert, J. *Physical Review B*, **1999**, 59, 1758.

42.- Monkhorst, H. J.; Pack, J. D. *Physical Review B*, **1976**, 13, 5188-5192.

43.- Solovyev, I. V.; Anisimov, V. I.; Dederichs, P. H. *Phys. Rev. B*, **1994**, 50, 16861-16871.

44.- Anisimov, V. I.; Aryasetiawan, F.; Lichtenstein, A. I. *Journal of Physics:*

*Condensed Matter*, **1997**, 9, 767.

45.- Dudarev, S. L.; Botton, G. A.; Savrasov, S. Y.; Humphreys, C. J.; Sutton, A. P., *Phys. Rev. B*, **1998**, 57, 1505.

46.- Calzado, C. J.; Hernández, N. C.; Fernández-Sanz, J. ; *Phys. Rev. B*, **2008**, 77, 045118.

47.- Pearse, RWB; Gaydon, AG, *The identification of molecular spectra*, Chapman & Hall Ltd, London **1950**.

48.- Suraj, KS; Bharathi, P; Prahlad, V.; Mukherjee, S., *Surf. Coat. Technol.* **2007**, 202, 301.

49.- Romero-Gómez, P.; Barranco, A.; Cotrino, J.; Espinós, J.P.; Yubero, F.; González-Elipe, A.R., *Plasma Deposition of N-$TiO_2$ thin Films, i*n "Industrial Plasma Technology. Applications from Environmental to Energy Technologies". Y. Kawai, Y.; Ikegami, H.; Sato, N.; Matsuda, A.; Uchino, K.; Kuzuya, M.; Mizuno, A., edts.; Wiley. Weinhaim **2010**. pag.349

50.- G. Lassaletta, G.; Fernández, A.; Espinós, J.P.; González-Elipe, A.R., *J. Phys. Chem*. **1995**, *99*, 1484

51.- Cong, Y.; Zhang, J.; Anpo, M. J. Phys. Chem. C **2007,** 111, 6979

52.- López-Luke, T.; Wolcott, A.; Xu, L-p.; Chen, Sh.; Wen, Z.; Li, J.; de la Rosa, E.; Zhang, J.Z., *J. Phys. Chem. C* **2008,** 112, 1282.

53.- Asahi, R.; Morikawa, T.; Hazama, H.; Matsubara, M., *J. Phys. Condens. Matter* **2008,** 20, 064227

54.-Batzill, M; Morales, E.H.; Diebold, U., *Phys. Rev. Lett.,* **2006**, 96, 026103

55.-Chen, H.; Nambu, A.; Wen, W.; Graciani, J.; Zhong, Z.; Hanson, J.C.; Fujita, E.; Rodriguez, J.A., *J. Phys. Chem. C* **2007**, 111, 1366

56.-Dunnill, C.W.H.; Aiken, Z.A.; Pratten, J.; Wilson, M.; Morgan, D.J.; Parkin, I.P., *J. Photochem. Photobiol. A. Chemistry,* **2009**, 207, 244

57.- Saha, N.C.; Tompkins, H.G., *J. Appl. Phys.,***1992**, 72, 3072

58.- Swanepoel, R. *J. Phys. E* 1983, 16, 1213.

59.- Irie, H.; Washizuka, S.; Watanabe, Y.; Kako, T.; Hashimoto, K. *J. Electrochem. Soc.* **2005,** 152 , E351

60.- Serpone, N.; Lawless, D.; Khairutdinov, R. *J. Phys. Chem.* **1995,** 99, 16646.

61.- Martin, N.; Besnard, A.; Sthal, F.; Vaz, F.; Nouveau, C. *Appl. Phys. Lett*. **2008**, 93, 064102.

62.- Zhu, J.; Ren J.; Huo Y.; Bian Z., *J. Phys. Chem C.* **2007**, 111, 18965.

63.- Finazzi, E.; di Valentin, C.; Pacchioni, G.; Selloni, A.; J. Chem. Phys. **2008**, 129, 154113

64.- Rico, V.; Romero-Gomez, P.; J.L.Hueso, J.L.; J.P.Espinós, J.P.; González-Elipe, A.R., *Catal. Today* **2009**, 143, 347

Table 1.- Relevant distances (in Å) involved in the three types of defects studied: $N_i$, $N_s$ and $N_{si}$. The distance between the two defects in the unit cell is taken into account by labeling with C and S the structures in which the N atoms are close and separated respectively.

| **Species** | **O-Ti** | **N-O** | **N-Ti** |
|---|---|---|---|
| $N_i$**-C** | 2.06, 2.06, 2.01 | 1.48 | 1.95, 1.98, 2.05 |
| $N_i$**-S** | 2.13, 2.13, 2.28 | 1.36 | 2.06, 2.06, 2.28 |
| $N_S$**-C** | | | 1.98, 2.00, 2.07 |
| $N_S$**-S** | | | 2.00, 2.00, 2.09 |
| $N_{Si}$**-C** | 2.09, 2.17, 3.33 | 1.29 | 1.98, 2.02, 2.04 |
| $N_{Si}$**-S** | 2.17, 2.17, 3.30 | 1.28 | 2.02, 2.03, 2.03 |

**Figure captions.-**

Fig. 1.- Schematic representation of the Ti precursors utilized for the synthesis of the N-$TiO_2$ thin films by plasma deposition.

Fig. 2.- N1s spectra recorded for a series of N-$TiO_2$ thin films prepared with the TDMAT precursor and different percentages of $N_2$ in the plasma as indicated. Note that some spectra are affected by a multiplication factor to bring them into a common scale.

Figure 3.- Fitted (gray line) and experimental (black line) N1s normalized spectra of selected N-$TiO_2$ thin films prepared at 523 K with the TDMAT (left) and the TTIP (right) precursors and different percentages of $N_2$ in the plasma gas. Elemental bands used for fitting are plotted in gray.

Figure 4.- N/Ti ratio determined from the intensities of the N1s and Ti2p photoelectron peaks as a function of the percentage of nitrogen in the $O_2$+$N_2$ mixture used as plasma gas. The dashed line is included to guide the eyes.

Figure 5.- Set of absorption spectra recorded for a series of N-$TiO_2$ thin films prepared at 523 K with the TDMAT precursor and different percentages of nitrogen in the plasma gas as indicated in each particular panel. The gray color spectrum included for comparison in each panel corresponds to the absorption spectrum of a pure $TiO_2$ thin film.

Figure 6.- Values of the absorption threshold plotted against the percentage of nitrogen in the plasma gas for N-$TiO_2$ thin films prepared with the TTIP, TDMAT and TDMAT precursors at 523 K. The dashed line is included to guide the eyes.

Figure 7.-Top) Refraction index and bottom) extinction coefficient curves determined for N-$TiO_2$ thin films prepared at 523 K by using TDMAT as a precursor and different percentages of $N_2$ in the mixture used as plasma gas as indicated. The star points to the region whose reproduction is only possible by admitting an oscillator around 375 nm.

Figure 8.- Structures of the three type of N centers studied. a) Substitutional defect, $N_s$, in which a N atom replaces a O atom. b) Interstitial defect, $N_i$, in which the N atom is located in an interstitial place, and the O atom is also displaced from its original site. c) Substitutional-interstitial defect, $N_{si}$, in which the N atom occupies the same position as in the case of the $N_s$ defect, and the O atom occupies an interstitial place.

Figure 9.- Density of states plots of the six N-$TiO_2$ systems studied, showing the two spin components separately. **a** and **b** correspond to the two systems with substitutional

N doping ($N_s$), with 2 N atoms located at close and separated positions, respectively. **c** and **d** correspond to the two systems with interstitial N doping ($N_i$), with 2 N atoms located at close and separated positions, respectively, respectively. **e** and **f** correspond to the two substitutional-interstitial N configurations ($N_{si}$), with 2 N atoms located at close and separated positions, respectively, respectively. The bands are plotted in such a way that the origin of the energy (0 eV) is placed at the bottom of the conduction band. The two vertical dashed lines are placed to indicate HOMO-LUMO gap in $TiO_2$. The vertical solid line indicate the highest occupied orbital of the system, which in the case of N-$TiO_2$ corresponds to new gap states generated by the presence of nitrogen in the lattice.

Figure 10.- Partial density of states plots of N, Ti and O in the gap states for the six studied N-$TiO_2$ systems with the labelling a)-f) being the same than in Fig. 9. The oxygen contribution is differentiated for the oxygen atoms close to the nitrogen and the rest of oxygen atoms of the lattice. The total densities of states plotted in Figure 9 are calculated as the sum of these partial densities of states. The vertical solid line indicates the highest occupied orbital of the system.

Figure 11.- Evolution of the wetting angle as a function of the illumination time with visible and UV lights and then left in the dark for N-$TiO_2$ samples prepared with 85% (top) and 97% (bottom) of $N_2$ in the plasma gas. The lines are plotted to guide the eyes.

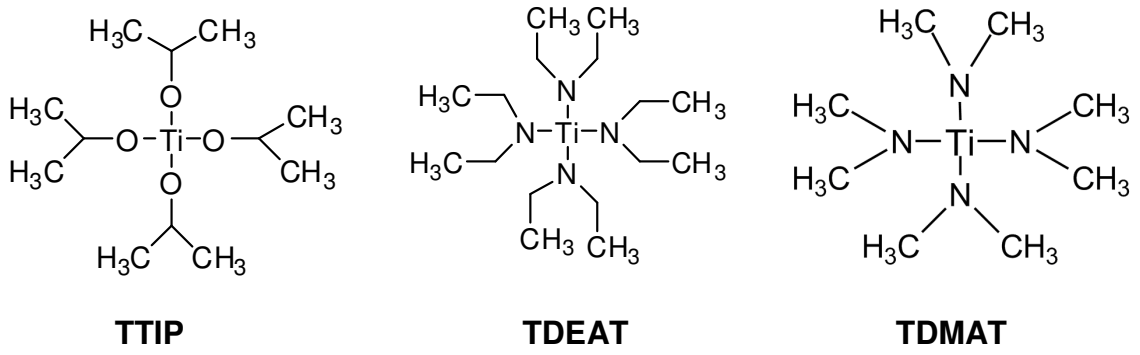

**TTIP** **TDEAT** **TDMAT**

**TTIP: titanium tetrakis isopropoxide**

**TDEAT: tetrakis diethyl amino titanium**

**TDMAT: tetrakis dimethyl amino titanium**

Fig. 1.- Schematic representation of the Ti precursors utilized for the synthesis of the N-$TiO_2$ thin films by plasma deposition.

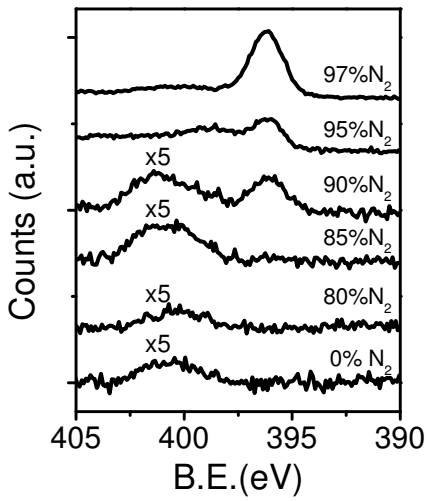


Fig. 2.- N1s spectra recorded for a series of N-$TiO_2$ thin films prepared with the TDMAT precursor and different percentages of $N_2$ in the plasma as indicated. Note that some spectra are affected by a multiplication factor to bring them into a common scale.

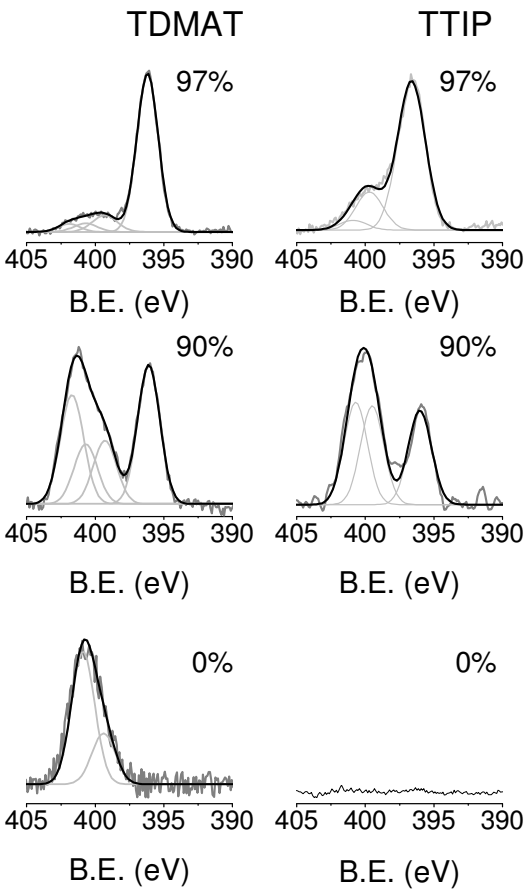


Figure 3.- Fitted (gray line) and experimental (black line) N1s normalized spectra of selected N-$TiO_2$ thin films prepared at 523 K with the TDMAT (left) and the TTIP (right) precursors and different percentages of $N_2$ in the plasma gas. Elemental bands used for fitting are plotted in gray.

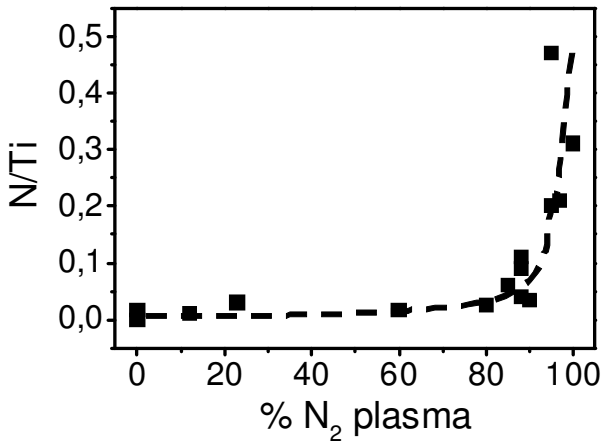


Figure 4.- N/Ti ratio determined from the intensities of the N1s and Ti2p photoelectron peaks as a function of the percentage of nitrogen in the $O_2$+$N_2$ mixture used as plasma gas. The dashed line is included to guide the eyes.

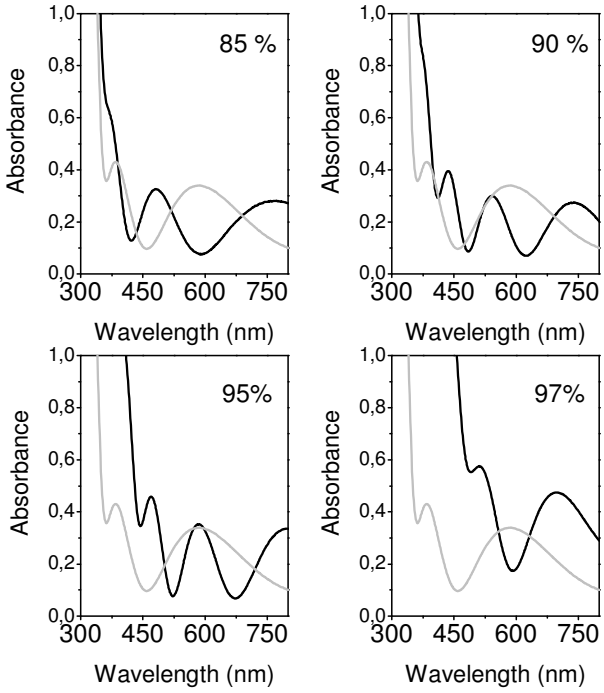


Figure 5.- Set of absorption spectra recorded for a series of N-$TiO_2$ thin films prepared at 523 K with the TDMAT precursor and different percentages of nitrogen in the plasma gas as indicated in each particular panel. The gray color spectrum included for comparison in each panel corresponds to the absorption spectrum of a pure $TiO_2$ thin film.

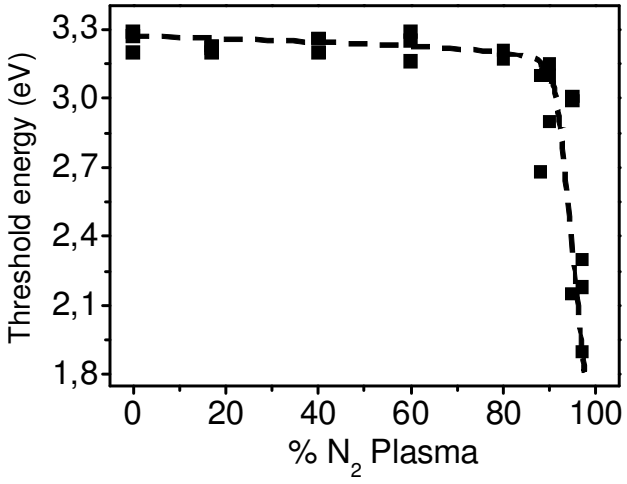


Figure 6.- Values of the absorption threshold plotted against the percentage of nitrogen in the plasma gas for N-$TiO_2$ thin films prepared with the TTIP, TDMAT and TDMAT precursors at 523 K. The dashed line is included to guide the eyes.

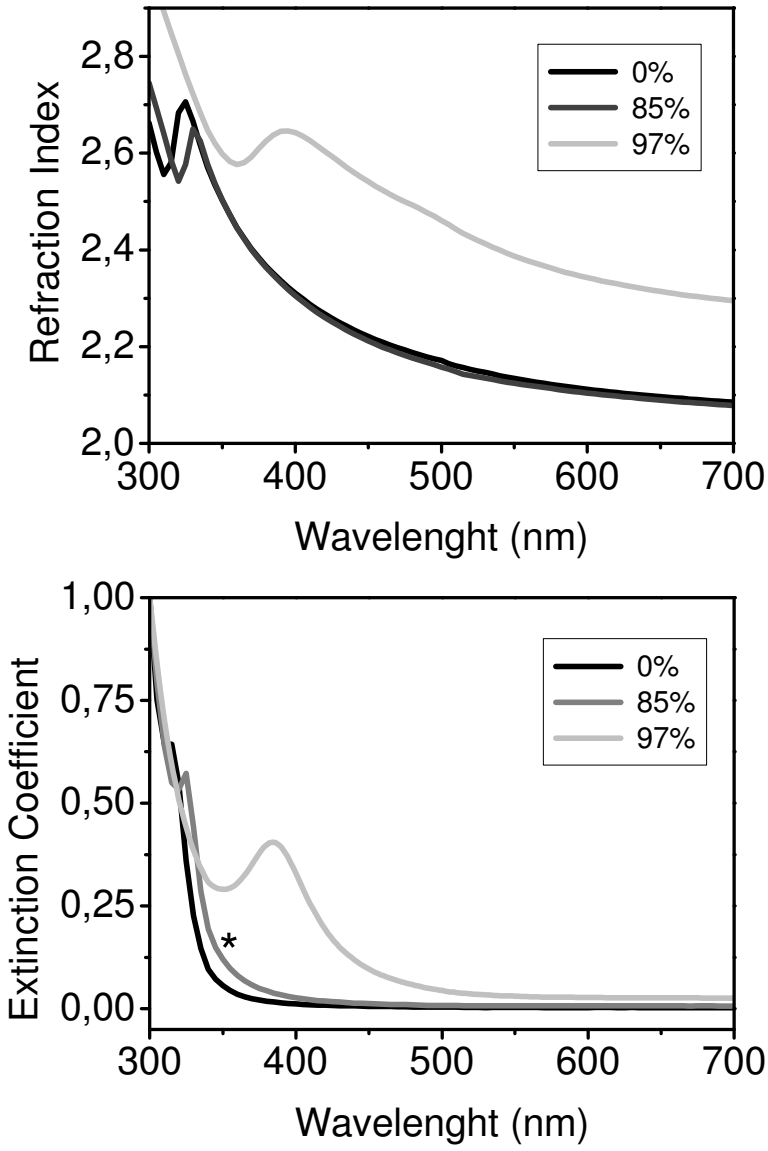


Figure 7.-Top) Refraction index and bottom) Extinction coefficient curves determined for N-$TiO_2$ thin films prepared at 523 K by using TDMAT as a precursor and different percentages of $N_2$ in the mixture used as plasma gas as indicated. The star points to the region whose reproduction is only possible by admitting an oscillator around 375 nm.

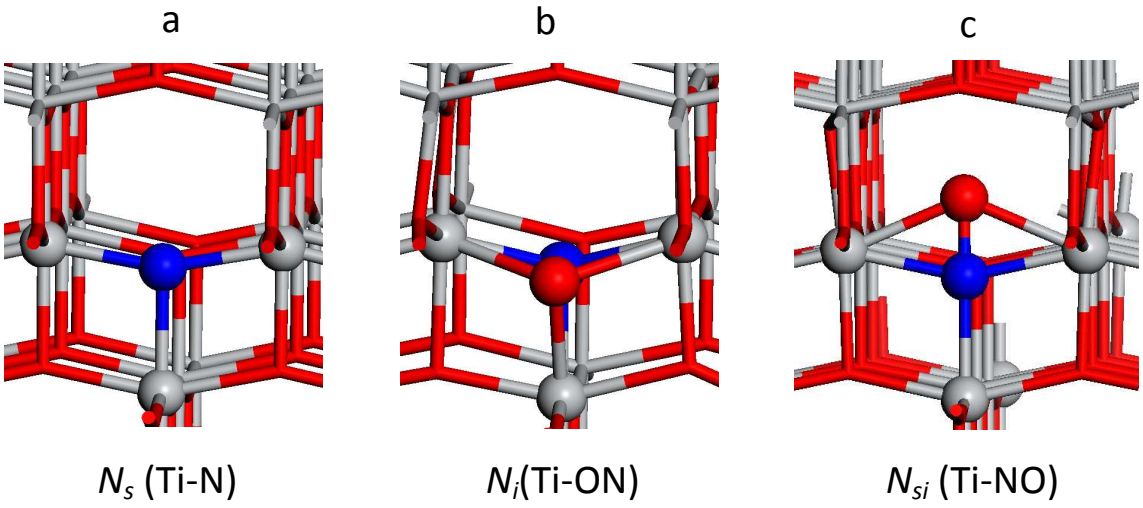


Figure 8.- Structures of the three type of N centers studied. a) Substitutional defect, $N_s$, in which a N atom replaces a O atom. b) Interstitial defect, $N_i$, in which the N atom is located in an interstitial place, and the O atom is also displaced from its original site. c) Substitutional-interstitial defect, $N_{si}$, in which the N atom occupies the same position as in the case of the $N_s$ defect, and the O atom occupies an interstitial place.

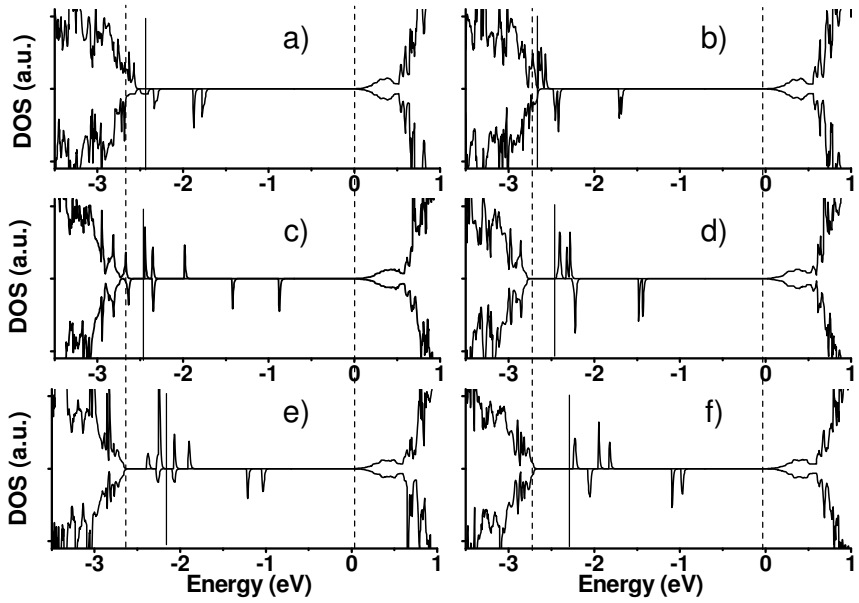


Figure 9.- Density of states plots of the six N-$TiO_2$ systems studied, showing the two spin components separately. **a** and **b** correspond to the two systems with substitutional N doping ($N_s$), with 2 N atoms located at close and separated positions, respectively. **c** and **d** correspond to the two systems with interstitial N doping ($N_i$), with 2 N atoms located at close and separated positions, respectively, respectively. **e** and **f** correspond to the two substitutional-interstitial N configurations ($N_{si}$), with 2 N atoms located at close and separated positions, respectively, respectively. The bands are plotted in such a way that the origin of the energy (0 eV) is placed at the bottom of the conduction band. The two vertical dashed lines are placed to indicate HOMO-LUMO gap in $TiO_2$. The vertical solid line indicate the highest occupied orbital of the system, which in the case of N-$TiO_2$ corresponds to new gap states generated by the presence of nitrogen in the lattice.

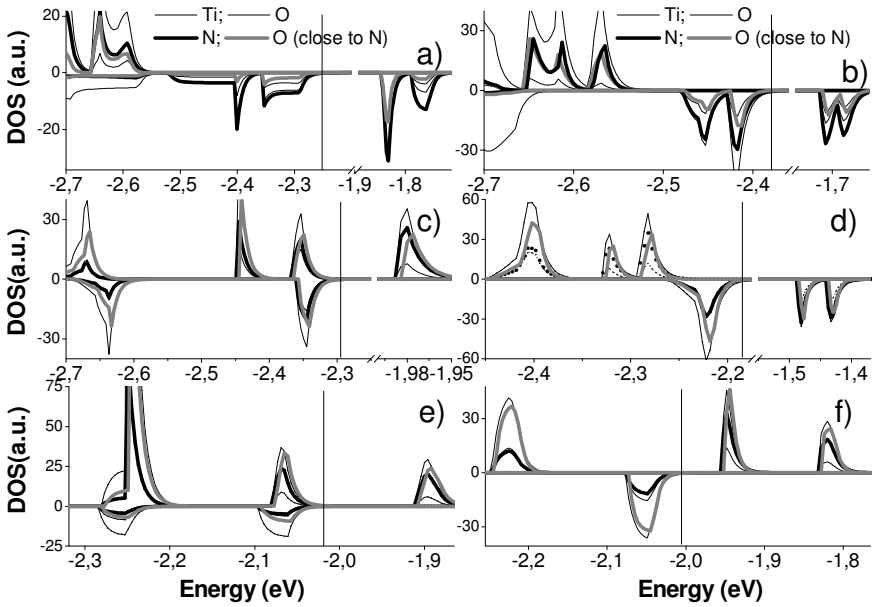


Figure 10.- Partial density of states plots of N, Ti and O in the gap states for the six studied N-$TiO_2$ systems with the labelling a)-f) being the same than in Fig. 9. The oxygen contribution is differentiated for the oxygen atoms close to the nitrogen and the rest of oxygen atoms of the lattice. The total densities of states plotted in Figure 9 are calculated as the sum of these partial densities of states. The vertical solid line indicates the highest occupied orbital of the system.

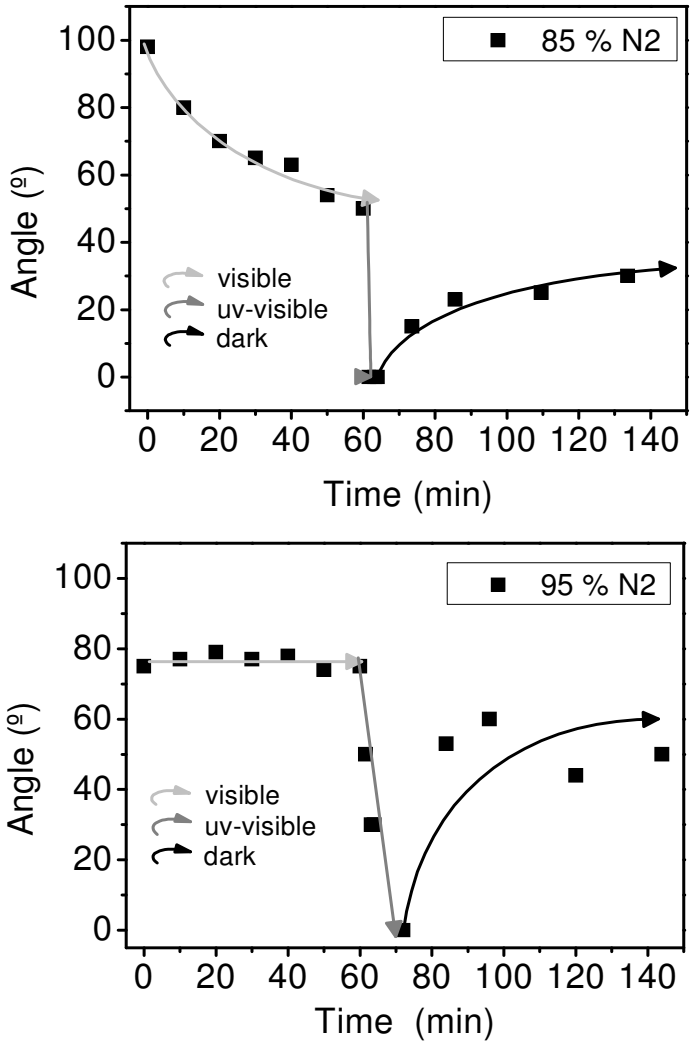


Figure 11.- Evolution of the wetting angle as a function of the illumination time with visible and UV lights and then left in the dark for N-$TiO_2$ samples prepared with 85% (top) and 97% (bottom) of $N_2$ in the plasma gas. The lines are plotted to guide the eyes.

## Table of Contents Image